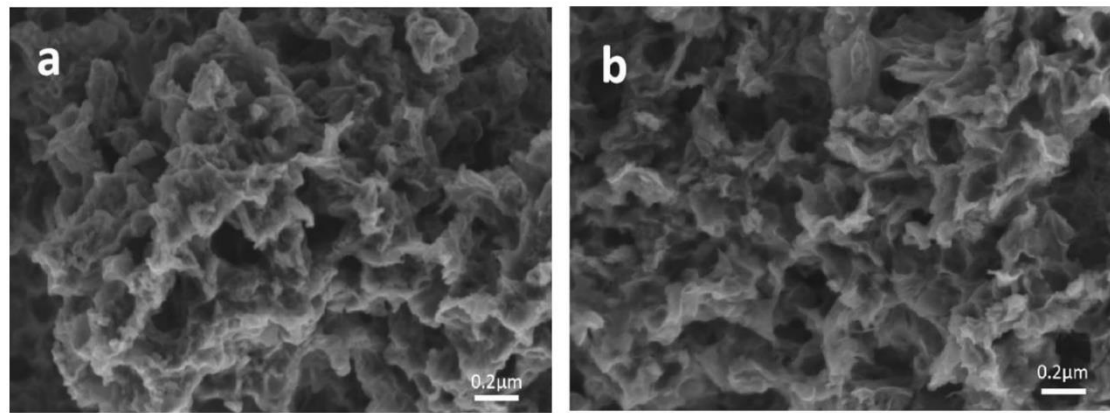


## Supporting Information

### **Design and synthesis Few-layer Molybdenum Oxide Selenide Encapsulated in 3D interconnected nitrogen-doped carbon Anode Toward High-Performance sodium storage**

Yonghong Qin<sup>1, 2</sup>, Shahriman Zainal Abidin<sup>1\*</sup>, Azhari Bin Md Hashim<sup>1</sup>, Oskar Hasdinor Hassan<sup>1</sup>, and Xiaojun Zhao<sup>3\*</sup>



**Fig. S1** SEM images of (a) MoO<sub>3</sub>-NC and (b) MoSe<sub>2</sub>-NC.

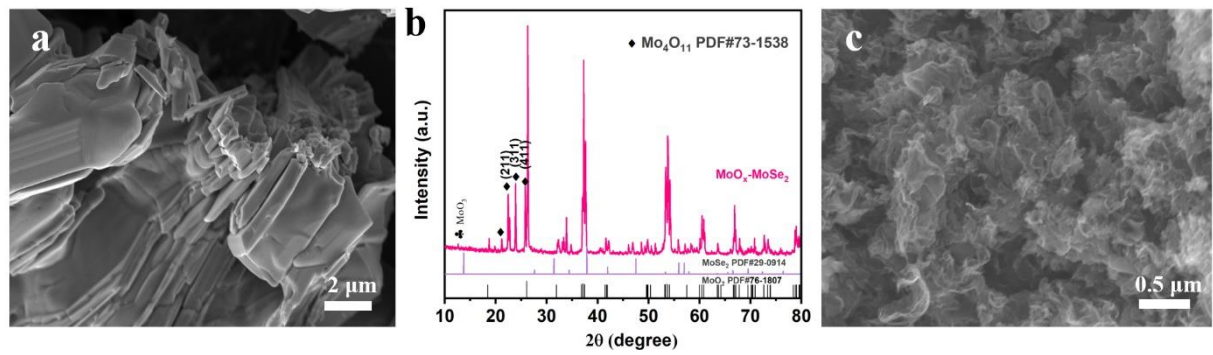


**Fig. S2** SEM images of (a) MoO<sub>x</sub>-MoSe<sub>2</sub> and (b) NC.

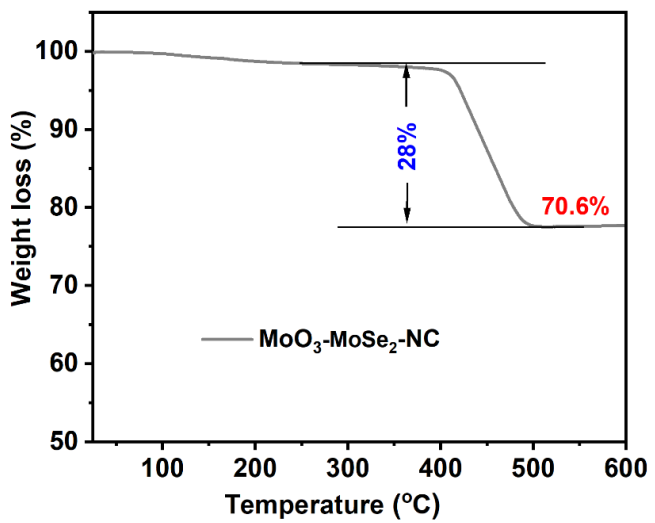


**Fig. S3** TGA curves of  $\text{MoO}_3\text{-MoSe}_2\text{-NC}$ .

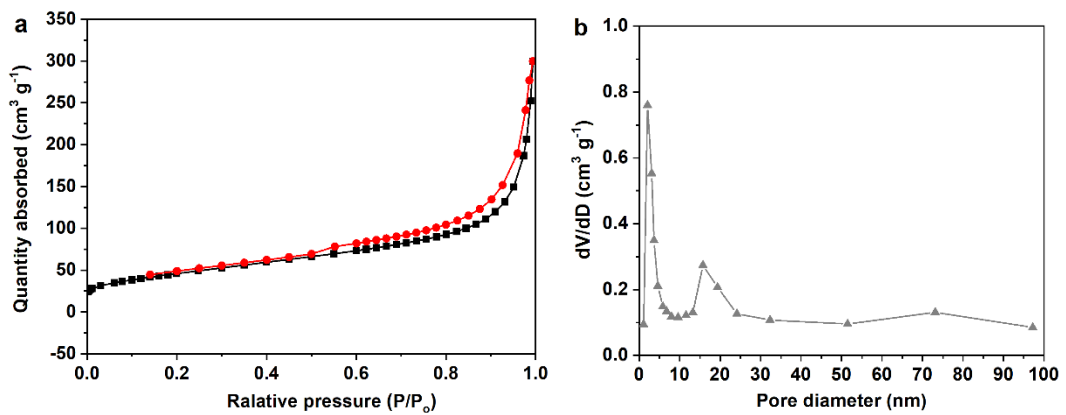


**Fig. S4** (a)  $\text{N}_2$  adsorption-desorption isotherms and (b) the pore-size distribution plot of the TGA curves of  $\text{MoO}_3\text{-MoSe}_2\text{-NC}$ .

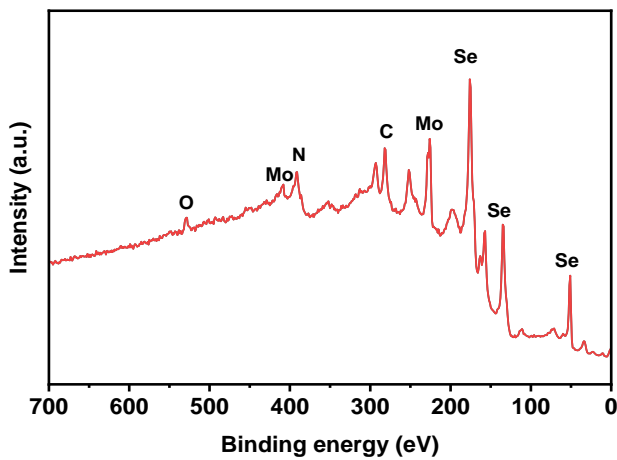


**Fig. S5** XPS survey of  $\text{MoO}_3\text{-MoSe}_2\text{-NC}$ .

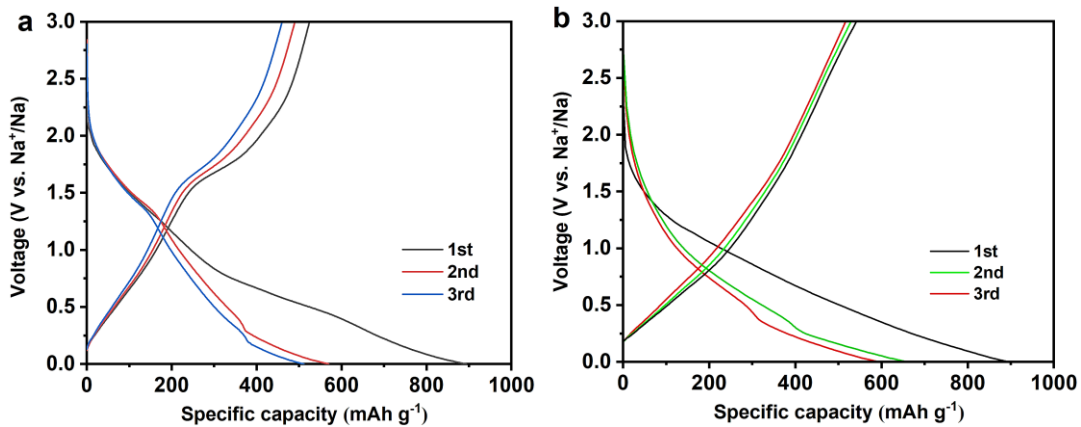


**Fig. S6** Galvanostatic discharge/charge curves of (a)  $\text{MoSe}_2\text{-NC}$  and (b)  $\text{MoO}_3\text{-NC}$ , respectively.

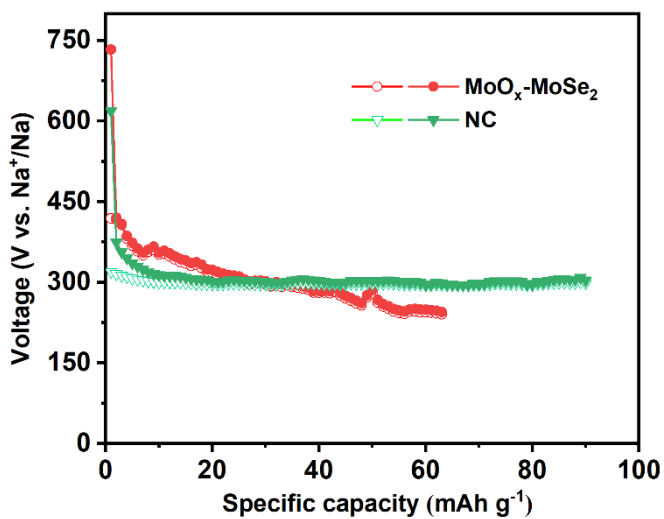


**Fig. S7** Cycle performance of MoO<sub>x</sub>-MoSe<sub>2</sub> and NC at 0.1 A g<sup>-1</sup>.

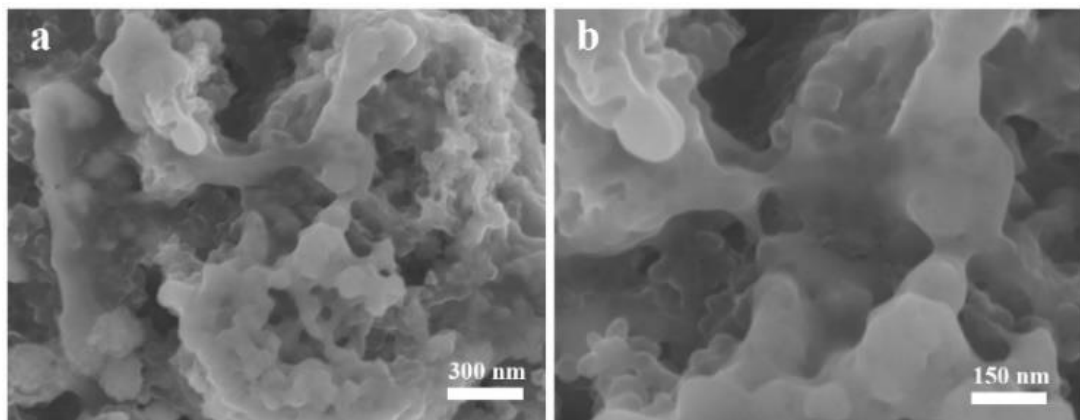


**Fig. S8 (a, b)** SEM images of MoO<sub>3</sub>-MoSe<sub>2</sub>-NC sample after 100 cycles for SIBs.

**Table S1** Performance comparison between MoO<sub>3</sub>-MoSe<sub>2</sub>-NC anode and the reported anode materials for SIBs

Samples	Cycle performance (mAh g <sup>-1</sup> )/number	Current density (A g <sup>-1</sup> )	Ref.
	551/150 368/600	0.1 1	
<b>MoO<sub>3</sub>-MoSe<sub>2</sub>-NC</b>			<b>This work</b>
<b>MoO<sub>2</sub>/MoSe<sub>2</sub>-graphene</b>	404 (rate capability) 340/300	0.1 0.5	<i>Energy Storage Materials</i> , 2018, 12, 241-251
<b>MoSe<sub>2</sub> nanoparticles</b>	374/100	0.5	<i>J. Alloys. Compds.</i> 2022, 922, 166306
<b>MoSe<sub>2</sub>@C HNS</b>	458/200	0.5	<i>Inorg. Chem. Front.</i> , 2020, 7, 1691-1698
<b>MoSe<sub>2</sub>@NPC/rGO</b>	340/500	0.5	<i>J. Power Sources</i> , 2020, 476, 228660
<b>TiO<sub>2</sub>@MoO<sub>2</sub>-C</b>	210/500	1	<i>Adv. Energy Mater.</i> 2017, 7(15), 1602880
<b>MoO<sub>2</sub>/MoSe<sub>2</sub>@NPC</b>	382/200	0.1	<i>ACS Appl. Mater. Interfaces</i> 2022, 14, 32, 36592–36601

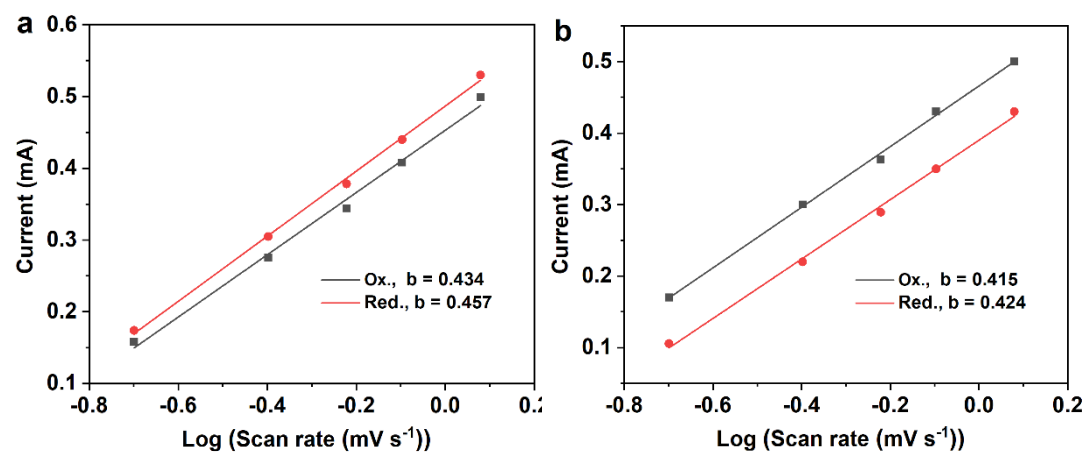


**Fig. S9** Linear relation between  $I_p$  and  $v^{1/2}$  of the (a) MoO<sub>3</sub>-MoSe<sub>2</sub>-NC and (b) MoSe<sub>2</sub>-NC anodes for SIBs, respectively.

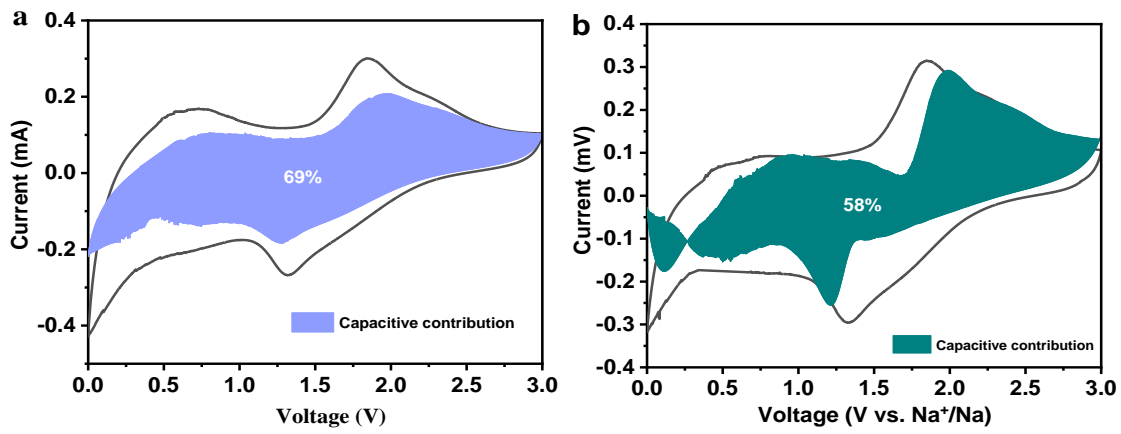


**Fig. S10** Separation of the capacitive and diffusion currents at a scan rate of 0.6 mV s<sup>-1</sup> of the (a) MoO<sub>3</sub>-MoSe<sub>2</sub>-NC and (b) MoSe<sub>2</sub>-NC anodes for SIBs, respectively.

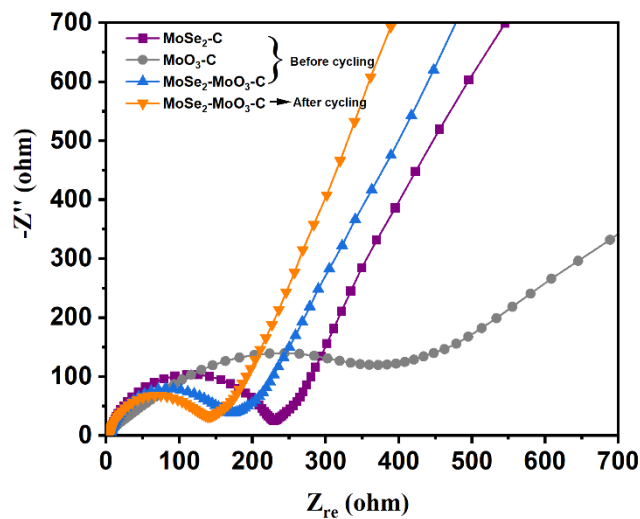


**Fig. S11** Nyquist plots of MoO<sub>3</sub>-MoSe<sub>2</sub>-NC, MoSe<sub>2</sub>-NC, and MoO<sub>3</sub>-NC anodes before and after cycling.